Rapid Communications

Experimental observation of conditional past-future correlations

Shang Yu,[1,2] Adrián A. Budini,[3] Yi-Tao Wang,[1,2] Zhi-Jin Ke,[1,2] Yu Meng,[1,2] Wei Liu,[1,2] Zhi-Peng Li,[1,2] Qiang Li,[1,2] Zheng-Hao Liu,[1,2] Jin-Shi Xu,[1,2] Jian-Shun Tang,[1,2,*] Chuan-Feng Li,[1,2,†] and Guang-Can Guo[1,2]

[1]*CAS Key Laboratory of Quantum Information, University of Science and Technology of China, Hefei 230026, China*

[2]*CAS Center For Excellence in Quantum Information and Quantum Physics, University of Science and Technology of China, Hefei 230026, China*

[3]*Consejo Nacional de Investigaciones Científicas y Técnicas (CONICET), Centro Atómico Bariloche, Avenida E. Bustillo Km 9.5, (8400) Bariloche, Argentina and Universidad Tecnológica Nacional (UTN-FRBA), Fanny Newbery 111, (8400) Bariloche, Argentina*

(Received 3 June 2019; published 8 November 2019)

Conditional past-future correlations measure the lack of statistical independence between past and future system measurement outcomes when conditioned to a given state at a present time. Quantum non-Markovian memory effects are present whenever this correlation is not null. Conditional past-future correlations can also be used to detect initial system-environment correlated states. In this work, we provide theoretical and experimental evidence for these general properties. We build an optical setup that implements the dynamics of a qubit interacting with a dephasing spin bath. Both finite and infinite bath-size limits are observed. Confirmation of theoretical predictions for conditional past-future correlations is obtained. This work provides experimental support for quantum memory indicators based solely on outcomes of explicit system measurement processes.

DOI: 10.1103/PhysRevA.100.050301

Introduction. In our daily experience, past and future events are highly correlated. This property, however, begins to weaken when the unpredictable influence of the environment over a system of interest becomes significant. A manageable and powerful mathematical description arises in the limit in which the probability of future events depends only on the current system state, being conditionally independent of its previous history. This classical memoryless *Markovian* property [1] can be rephrased in terms of a *conditional past-future independence*, in which past and future system events become statistically independent when conditioned to a given state at an intermediate present time [2]. Non-Markovian memory effects break these conditions.

In a quantum regime, the presence of memory effects is usually unrelated to previous probability settlements. In fact, the state of a quantum system depends on which way it is measured [3,4]. Thus, most of the proposed definitions of quantum Markovianity (and, consequently, quantum non-Markovianity) rely on information that is attainable only from the (unperturbed) system density matrix evolution [5,6]. Given the relevance of memory effects in quantum information devices, different experimental arrangements have been implemented to support diverse related theoretical formalisms [7–14]. Memory effects induced by initial system-environment correlations have also been studied on similar grounds from both theoretical and experimental points of view [15–29].

In contrast to previous approaches, definitions of quantum non-Markovianity that solely rely on information provided by subsequent measurement processes performed over the system of interest have recently been proposed [30–32]. Consistence with previous classical probability settlements is achieved. Owing to the lack of a preferential basis for the selection of possible observables at each stage, it is expected that the quantum nature of the dynamics gives rise to a richer structure when compared with the classical (incoherent) case. The aim of this Rapid Communication is to provide experimental support to these novel quantum-measurement-based formalisms and to explore which novel features may emerge due to the quantumness of the observed system.

In this work, we develop an experimental photonic platform for measuring the conditional past-future (CPF) correlation of a qubit system that interacts with a dephasing spin bath [32]. The CPF correlation measures the break of CPF independence, which is only valid in the memoryless Markovian regime. Both finite and infinite bath sizes are implemented. In addition, we demonstrate both theoretically and experimentally that the CPF correlation, only when considering quantum systems, also allows witnessing initial system-environment correlations. Thus, this quantum signature allows one to unify the detection of both quantum memory effects and initial correlations in a single frame, which in contrast to previous approaches solely rely on system measurement outcomes. Our results also support the interpretation of CPF correlations in terms of a measurement back action on the environmental degrees of freedom [32].

Conditional past-future correlation. This object is determined by a minimal set of three measurement processes performed over the system of interest at three successive times $t_x < t_y < t_z$. Defining the system observables at the initial and final steps as $\{O_x\}$ and $\{O_z\}$, respectively, the CPF correlation

*tjs@ustc.edu.cn
†cfli@ustc.edu.cn

is obtained as follows:

$$C_{pf}(t,\tau) = \langle O_z O_x\rangle_y - \langle O_z\rangle_y \langle O_x\rangle_y, \tag{1}$$

where the time intervals are $t \equiv t_y - t_x$ and $\tau \equiv t_z - t_y$. The averages are conditioned to a y outcome of the intermediate measurement. Explicitly, the correlation is $C_{pf}(t,\tau) = \Sigma_{zx}[P(z,x|y) - P(z|y)P(x|y)]O_z O_x$, where the sum indices run over all possible outcomes at each stage. The conditional probabilities [33] follow from quantum measurement theory [4] by taking into account that each measurement process has associated a set of normalized operators, $\{\Omega_x\}$, $\{\Omega_y\}$, and $\{\Omega_z\}$.

In the same way as a classical regime, quantum Markovianity is defined by the statistical independence of past and future events when conditioned to a given state at the present time [$P(z,x|y) = P(z|y)P(x|y)$]. Thus, a system is Markovian if for arbitrary measurement operators $\{\Omega_x\}$, $\{\Omega_y\}$, and $\{\Omega_z\}$ the CPF correlation vanishes, $C_{pf}(t,\tau) = 0$. Equivalently, a system dynamics is non-Markovian if there exists at least one set of measurement operators $\{\Omega_x\}$, $\{\Omega_y\}$, and $\{\Omega_z\}$, such that $C_{pf}(t,\tau) \neq 0$. If memory effects are present, in general it is expected that a "continuous set of measurement processes" will give rise to a non-null CPF correlation. As stated in Ref. [32], this definition of non-Markovianity can be related to a measurement back action on the environment degrees of freedom that changes the system dynamics between consecutive measurements.

Detection of initial system-environment correlations. According to Ref. [32], a CPF correlation has the following properties [34]. It always vanishes when the time interval τ between the second and third measurements approaches zero [i.e., $\lim_{\tau\to 0} C_{pf}(t,\tau) = 0$]. However, for the complementary limit where the time interval t between the first and second measurements approaches zero, the CPF correlation vanishes whenever the initial system-environment state ρ_0^{se} is an uncorrelated one, namely,

$$\rho_0^{se} = \rho_0 \otimes \sigma_e \;\Rightarrow\; \lim_{t\to 0} C_{pf}(t,\tau) = 0. \tag{2}$$

From this property, we can derive a criterion for detecting initial system-environment correlations that is similar to the previous one for quantum non-Markovianity. The system and the environment are correlated at the initial time if there exists at least one set of measurement operators $\{\Omega_x\}$, $\{\Omega_y\}$, and $\{\Omega_z\}$, such that $\lim_{t\to 0} C_{pf}(t,\tau) \neq 0$. Similarly, system and environment are uncorrelated at the initial time if, for arbitrary measurement operators $\{\Omega_x\}$, $\{\Omega_y\}$, and $\{\Omega_z\}$, $\lim_{t\to 0} C_{pf}(t,\tau) = 0$.

The criterion based on Eq. (2) relies on the *quantumness of the observed system*. In fact, for classical systems the base for measurement observables is always the same (pointer states), in particular $\{\Omega_x\} = \{\Omega_y\}$. Consequently, when $t \to 0$ the outcomes of the first two measurements are identical, $\{x = y\}$. Thus, $\lim_{t\to 0} P(y|x) = \delta_{y,x}$. From the general result $P(z,x|y) = P(z|y,x)P(x|y) = P(z|y,x)P(y|x)P(x)/P(y)$, using the previous limit, it follows that $\lim_{t\to 0} P(z,x|y) = \lim_{t\to 0} P(z|y) \lim_{t\to 0} P(x|y)$. Thus, independently of the existence of initial correlations, it is always the case that $\lim_{t\to 0} C_{pf}(t,\tau) = 0$. In contrast, in quantum systems one can always select $\{\Omega_x\} \neq \{\Omega_y\}$, which in turn permits the detection of initial correlations from the CPF correlation, $\lim_{t\to 0} C_{pf}(t,\tau) \neq 0$.

Dephasing spin bath. As a dynamics to experimentally study the previous properties, we consider a qubit system (base $|+\rangle$ and $|-\rangle$) interacting with a quantum N-spin bath [35–37] via the dephasing Hamiltonian

$$H_T = \sigma_{\hat{z}} \otimes \sum_{k=1}^{N} g_k \sigma_{\hat{z}}^{(k)}. \tag{3}$$

Here, $\sigma_{\hat{z}}$ and $\sigma_{\hat{z}}^{(k)}$ are z-Pauli matrices for the system and the kth bath spin, respectively. g_k are coupling constants. The three measurements that define the CPF correlation are taken as projective ones, being performed in the $\hat{x}$ direction in the Bloch sphere of the qubit. The observables are $O_z = z$, $O_x = x$, where $z = \pm 1$ and $x = \pm 1$. This model, as well as the CPF correlation, admits a full exact analytical treatment (see Ref. [32]).

For an uncorrelated pure initial system-bath state $|\Psi_0\rangle = (a|+\rangle + b|-\rangle) \otimes |\mathcal{B}(0)\rangle$, at time t the Hamiltonian H_T leads to the state $|\Psi_t\rangle = a|+\rangle \otimes |\mathcal{B}(t)\rangle + b|-\rangle \otimes |\mathcal{B}(-t)\rangle$, with the bath state $|\mathcal{B}(t)\rangle = \prod_{k=1}^{N}(\alpha_k e^{+ig_k t}|\uparrow\rangle_k + \beta_k e^{-ig_k t}|\downarrow\rangle_k)$. Here $|\uparrow\rangle_k$ and $|\downarrow\rangle_k$ define the k-spin basis. $|\Psi_t\rangle$ can be rewritten as follows [37]:

$$|\Psi_t\rangle = \sum_{n=0}^{2^N-1} c_n (a|+\rangle e^{i\phi_n t} + b|-\rangle e^{-i\phi_n t}) \otimes |n\rangle. \tag{4}$$

The kth digit n_k of the binary form of the number n represents the state up ($n_k = 1 \leftrightarrow |\uparrow\rangle_k$) or down ($n_k = 0 \leftrightarrow |\downarrow\rangle_k$) of the k spin from the bath. The phases are $\phi_n = \sum_{k=1}^{N}(-1)^{n_k} g_k$. Equation (4) motivates the following optical implementation. The system states are encoded in the horizontal (H) and vertical (V) polarization light states ($|+\rangle \leftrightarrow |H\rangle$, $|-\rangle \leftrightarrow |V\rangle$), and 2^N spatial light modes are required to represent the environment. Therefore, two spatial light modulators (SLMs), each acting on each polarization component, introduce the phases $e^{i\phi_n t}$ and $e^{-i\phi_n t}$. As in Ref. [32], we take $g_k = g/\sqrt{N}$, and initials $\alpha_k = \beta_k = 1/\sqrt{2} \to c_n = 1/2^{N/2}$.

Experimental setup. The specific experimental setup for measuring the CPF correlation is illustrated in Fig. 1. It can be divided into five parts. Module (i) is a single-photon source; an additional heralded single photon is generated by a type-II spontaneous parametric down-conversion process in a beta-barium borate (BBO) crystal. In module (ii), the photon is sent to a polarization beam splitter (PBS) and a half-wave plate (HWP) to initialize its polarization state. The photon beam is expanded with a pair of lenses and passed through a digital mirror device (DMD), which generates 2^N identical pieces to represent the environmental states ($|n\rangle$). Module (iii) is inserted for preparing initial (system-environment) correlated states; this is achieved by inducing the full system-environment unitary dynamics (SLM A and SLM B) before the next step. In module (iv), two dephasing spin bath channels are placed between the first and second projective measurements, $\{\Omega_x\}$ and $\{\Omega_y\}$, and between the second and third projective measurements, $\{\Omega_y\}$ and $\{\Omega_z\}$. Each measurement is performed by a PBS sandwiched by a pair of HWPs. The dephasing dynamics [Eq. (4)] is realized by two SLMs that can adjust the phases on every 2^N spatial environment piece.

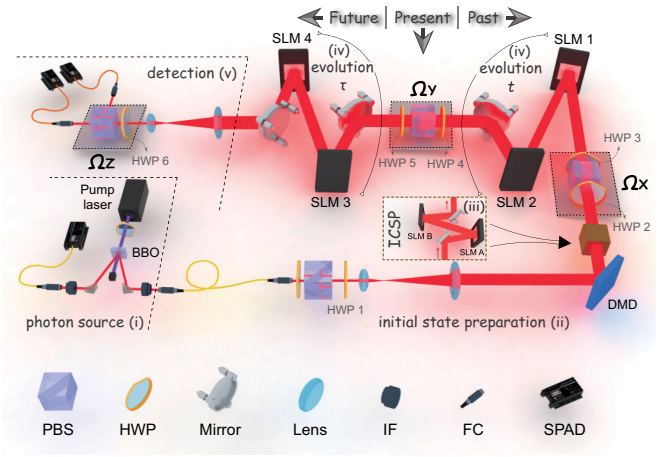

FIG. 1. The experimental setup for measuring the CPF correlation consists of five modules: (i) the single-photon source; (ii) preparation of initial system-bath states; (iii) the initial correlated states preparation (ICSP); (iv) dephasing dynamics between measurements; and (v) detecting devices for conditional probabilities. Projective measurements are performed by PBS Ω_x, Ω_y, and Ω_z. Key elements also include fiber coupler (FC) and interference filter (IF).

Here, SLM 1/3 responds to the horizontal polarization phase change, whereas SLM 2/4 responds to the vertical polarization phase change. In module (v), after the measurement $\{\Omega_z\}$, the photons are collected by multimode fibers and detected by single-photon avalanche detectors (SPADs). The conditional probabilities can be obtained by the total counts on each port: $P(z,x|y) = \mathcal{N}_{z,x|y}/\sum_{z',x'}\mathcal{N}_{z',x'|y}$, where $\mathcal{N}_{z,x|y}$ denotes the photon counts obtained after measurement $\Omega_{z=\pm} = |\hat{x}_\pm\rangle\langle\hat{x}_\pm|$, where $|\hat{x}_\pm\rangle = 1/\sqrt{2}(|+\rangle \pm |-\rangle)$. The first measurement is alternatively fixed at both $\Omega_{x=+} = |\hat{x}_+\rangle\langle\hat{x}_+|$ and $\Omega_{x=-} = |\hat{x}_-\rangle\langle\hat{x}_-|$. For the intermediate conditional measurement we can select $\Omega_{y=+} = |\hat{x}_+\rangle\langle\hat{x}_+|$ or $\Omega_{y=-} = |\hat{x}_-\rangle\langle\hat{x}_-|$.

The setup illustrated in Fig. 1 can, in principle, realize an arbitrary number of environmental spins and adjust the phase on each state $|n\rangle$ individually. In our experiment, limited by the screen size of the SLM, up to eight environmental spins can be prepared. To simulate the case in which $N =$ infinity, a slightly different scheme is implemented. All SLMs are applied as mirrors, and do not work for phase adjustment. A series of beam-displacing pairs is inserted into the setup to emulate the dephasing evolution [module (iv)] [10] and prepare the initial correlated states [module (iii)]. The other elements are the same as in the scheme depicted in Fig. 1. With a properly modulated spatial environment, Gaussian decay dependences are obtained, which in turn are equivalent to an infinite bath size [32]. Further details of this experimental setup are provided in [34].

Experimental results of CPF correlation. We first measure the CPF correlation to investigate the non-Markovian property of the system. According to the definition, the values of $C_{pf}(t,\tau)$ are determined by $P(z,x|y)$, $P(x|y) = \sum_{z=\pm1} P(z,x|y)$, and $P(z|y) = \sum_{x=\pm1} P(z,x|y)$. In this stage, we omit the initial correlations; hence module (iii) is not inserted into the setup. The initial polarization state is set to be $|H\rangle$. By adjusting the phase on SLM 1/2 and SLM 3/4 in each channel, we can vary the evolution time t and τ and scan the CPF correlation values.

The CPF correlation for $y = \pm1$ is [32] $C_{pf}(t,\tau) = f(t,\tau) - f(t)f(\tau)$, where $f(t,\tau) = [f(t+\tau) + f(t-\tau)]/2$, while $f(t) = \cos^N(2gt/\sqrt{N})$. Thus, for finite N, $C_{pf}(t,\tau)$ is a periodic function in both interval times (t,τ), with period $\pi\sqrt{N/4}/g$. Figure 2 presents the two-dimensional surface plots of $C_{pf}(t,\tau)$ in one period. Figures 2(a)– 2(c) are the analytical values for $N = 2$, 4, and 8, respectively, and Figs. 2(e)–2(g) are the corresponding experimental results. The CPF correlations change with the number of environmental spins and grow outward to an X-shaped form [32]. The location of the central peak (red area) increases

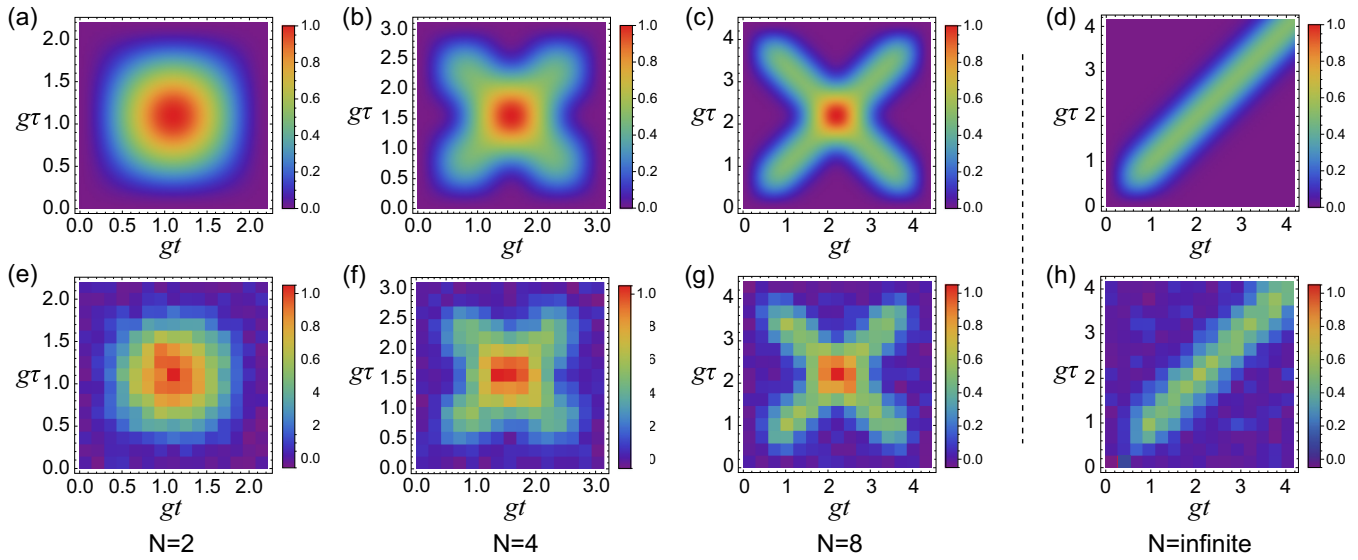

FIG. 2. CPF correlations for the spin-bath model (3) with different sizes, $N = 2,\ 4,\ 8$, and $N =$ infinite. (a)–(d) are the analytical results. (e)–(h) are the respective experimental results obtained from the proposed optical platform with a precision of 15×15 pixels in one period. The axes are the time intervals gt and $g\tau$ between successive measurements.

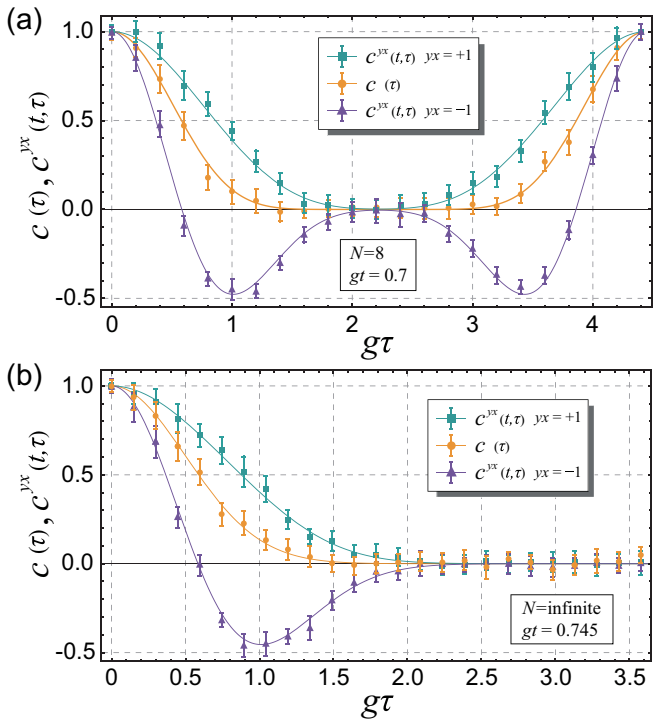

FIG. 3. System coherence behaviors $c(\tau)$ and $c^{yx}(t,\tau)$ between the first ($\{\Omega_x\}$ and $\{\Omega_y\}$) and last ($\{\Omega_y\}$ and $\{\Omega_z\}$) two measurements. (a) Finite spin bath with $N=8$. (b) Infinite bath size, $N=\infty$. Solid lines represent the theoretical predictions, and symbols represent experimental results.

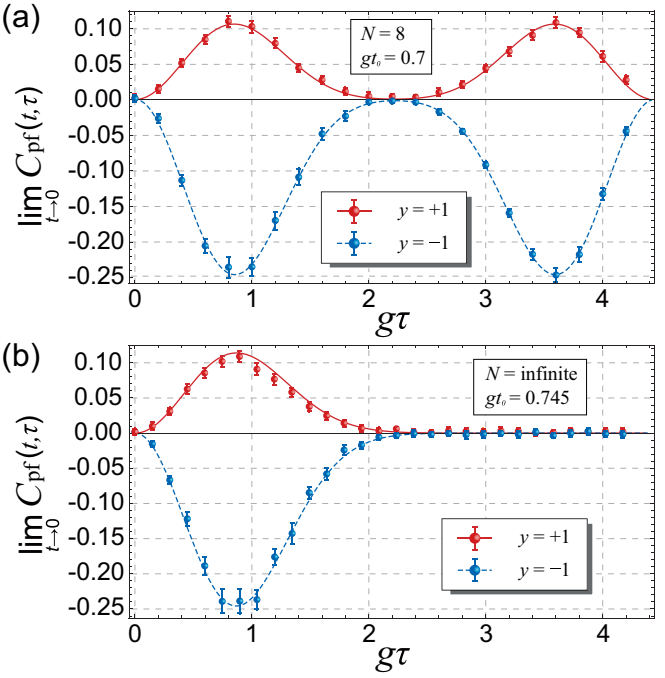

FIG. 4. CPF correlation for an initial system-environment correlated state induced by the total unitary dynamics during a time interval gt_0. (a) Finite bath, $N=8$. (b) Infinite bath size. In both cases, the symbols with error bars represent experimental results, and the solid lines are given by Eq. (5).

with N. In the limit $N\to\infty$ (d) and (h), which is performed with the alternative experimental scheme [34], CPF loses its periodicity (the location of the central peak diverges) and recovers a Gaussian behavior as presented in [32], $f(t)=\exp[-2(gt)^2]$. Consistently, the experimental results show that the environment correlation time is divergent, $\lim_{t\to\infty} C_{pf}(t,t)=1/2\neq 0$.

Coherence behavior between consecutive measurements. The quantum non-Markovianity indicated by a non-null CPF correlation (Fig. 2) can be read from a measurement back action on the environmental degrees of freedom, which in turn change the system dynamics between consecutive measurement events [32]. In fact, in the interval t, the bath starts in state $|\mathcal{B}(0)\rangle$, while the system coherence is $c(t)=\langle\mathcal{B}(-t)|\mathcal{B}(t)\rangle=[\cos(2gt/\sqrt{N})]^N$ $[c(t)=\exp[-2(gt)^2]$ for $N\to\infty]$. In contrast, in the interval τ, following the second measurement, the bath begins in state $|\mathcal{B}_{yx}(t)\rangle=[|\mathcal{B}(t)\rangle+yx|\mathcal{B}(-t)\rangle]/\sqrt{\mathcal{N}_t^{yx}}$, where $\mathcal{N}_t^{yx}$ is a normalization constant [32]. This *entangled spin bath state* depends on the outcomes product yx. This property translates to the system coherence behavior, which is $c^{yx}(t,\tau)=\langle\mathcal{B}_{yx}(t-\tau)|\mathcal{B}_{yx}(t+\tau)\rangle=[c_\tau+yx(c_{t+\tau}+c^*_{t-\tau})/2]/[1+yx(c_t+c_t^*)/2]$.

To verify this complementary reading of quantum non-Markovianity $[c(\tau)\neq c^{yx}(t,\tau)]$, we perform state tomography [38] at the first and second dephasing channel to obtain $c(t)$ and $c^{yx}(t,\tau)$, respectively. We plot these objects ($yx=\pm1$), for both finite ($N=8$) and infinite ($N=\infty$), bath size limits, Figs. 3(a) and 3(b), respectively. In both cases, $c(\tau)$ develops almost the same Gaussian behavior. However, for finite N periodic behavior is obtained. In contrast, the behavior of $c^{yx}(t,\tau)$ differs from $c(\tau)$ and in turn depends on the product $yx=\pm1$. These properties are consistent with theoretical predictions and also confirm the presence of memory effects as demonstrated in Fig. 2.

Initial correlated states. In order to introduce experimental initial correlated states, we submit an uncorrelated system-environment state to the total unitary dynamics during an effective time t_0 [module (iii) in Fig. 1]. This procedure entangles the qubit and the spin bath, $|\Psi_0\rangle=a|+\rangle\otimes|\mathcal{B}(t_0)\rangle+b|-\rangle\otimes|\mathcal{B}(-t_0)\rangle$. Consistent with our theoretical predictions, this initial correlation can be detected if the first two measurements are performed in different directions. As in the above setting, we maintain $\{\Omega_{x=\pm}\}=|\hat{x}_\pm\rangle\langle\hat{x}_\pm|$, $\{\Omega_{z=\pm}\}=|\hat{x}_\pm\rangle\langle\hat{x}_\pm|$, while now $\{\Omega_{y=\pm}\}=|\hat{n}_\pm\rangle\langle\hat{n}_\pm|$. Here, $\hat{n}$ is a direction in the $\hat{x}$-$\hat{z}$ plane in the Bloch sphere with polar angle θ. Thus, $|\hat{n}_\pm\rangle=\cos(\theta)|+\rangle\pm\sin(\theta)|-\rangle$. Using the parameters $a=b=1/\sqrt{2}$, it is possible to obtain the following [34]:

$$\lim_{t\to 0} C_{pf}(t,\tau)=y\frac{\cos^2(\theta)\sin(\theta)}{[1+yw\sin(\theta)]^2}[g(\tau)-wf(\tau)], \qquad (5)$$

where $g(t)=\mathrm{Re}[c(t_0+t)+c^*(t_0-t)]/2$, $f(t)=\mathrm{Re}[c(t)]$, and $w=\mathrm{Re}[c(t_0)]$. Consistently, for an uncorrelated initial state $[t_0=0]$, or when the first two measurements are performed in the same direction $[\theta=\pi/2]$, Eq. (5) leads to $\lim_{t\to 0} C_{pf}(t,\tau)=0$.

The previous expression can be tested by rotating the HWPs corresponding to $\{\Omega_y\}$ (see Fig. 1). In Fig. 4 we present the experimental results for both finite and infinite

bath sizes, and the two conditionals $y = \pm 1$. We set $\theta = 35.2^\circ$ [the angle that maximizes the global amplitude in Eq. (5)] and control SLM A, B such that $gt_0 = 0.7$. For finite N, the CPF correlation is periodic in τ (period $\sqrt{2}\pi$); this property is lost for $N =$ infinite (where $gt_0 = 0.745$). Whereas in Fig. 2, $\lim_{t\to 0} C_{pf}(t,\tau) = \lim_{\tau\to 0} C_{pf}(t,\tau) = 0$, here the property $\lim_{t\to 0} C_{pf}(t,\tau) \neq 0$ witnesses the initial system-environment correlations and illustrates the validity of the proposed approach. Complete experimental and theoretical plots of $C_{pf}(t,\tau)$ are shown in [34].

Conclusions. In summary, we have proposed a quantum optical arrangement that implements the dynamics of a qubit system interacting with a dephasing spin bath of variable size. The experimental setup allows determining correlations in the outcomes of successive projective measurements performed over the system. The results confirm the experimental detection of quantum non-Markovianity through nonvanishing CPF correlations. In addition, we have theoretically and experimentally demonstrated the ability of the CPF correlation method to detect initial system-environment correlations. This property relies on the quantumness of the observed system, which makes it possible to detect initial correlated states by selecting different bases for successive measurement processes. Furthermore, we have confirmed that memory effects follow from a measurement back action on the bath degrees of freedom that alters the system dynamics between consecutive measurements.

In contrast to previous approaches, CPF correlations provide a powerful alternative tool to study and detect quantum memory effects in a more intrinsic manner. In fact, the present approach solely relies on measurement outcomes performed over the system of interest. On the other hand, the optical setup may provide an experimental basis to study several other related topics of interest in the theory of non-Markovian open quantum systems together with their dependence on bath size. In fact, it can be applied as a distinctive all-optical simulator for many-body systems in future experiments and more general operations can be realized by this setup.

Acknowledgments. This work is supported by the National Key Research and Development Program of China (Grant No. 2017YFA0304100), the National Natural Science Foundation of China (Grants No. 61327901, No. 11674304, No. 11822408, No. 61490711, No. 11774335, and No. 11821404), the Key Research Program of Frontier Sciences of the Chinese Academy of Sciences (Grant No. QYZDY-SSW-SLH003), the Youth Innovation Promotion Association of Chinese Academy of Sciences (Grant No. 2017492), the Foundation for Scientific Instrument and Equipment Development of Chinese Academy of Sciences (Grant No. YJKYYQ20170032), Science Foundation of the CAS (Grant No. ZDRW-XH-2019-1), Anhui Initiative in Quantum Information Technologies (Grants No. AHY020100 and No. AHY060300), the National Postdoctoral Program for Innovative Talents (Grant No. BX20180293), China Postdoctoral Science Foundation funded project (Grant No. 2018M640587), and the Fundamental Research Funds for the Central Universities (Grant No. WK2470000026). A.A.B. acknowledges support from Consejo Nacional de Investigaciones Científicas y Técnicas (CONICET), Argentina.

S.Y. and A.A.B. contributed equally to this work.

[1] N. G. van Kampen, *Stochastic processes in physics and chemistry* (North-Holland, Amsterdam, 1981).

[2] T. M. Cover and J. A. Thomas, *Elements of Information Theory* (Wiley, New Jersey, 1991).

[3] H. P. Breuer and F. Petruccione, *The theory of open quantum systems* (Oxford University Press, Oxford, 2007).

[4] H. M. Wiseman and G. J. Milburn, *Quantum measurement and control* (Cambridge University Press, Cambridge, UK, 2010).

[5] H. P. Breuer, E. M. Laine, J. Piilo, and V. Vacchini, "*Colloquium*: Non-Markovian dynamics in open quantum systems", Rev. Mod. Phys. **88**, 021002 (2016).

[6] A. Rivas, S. F. Huelga, and M. B. Plenio, Quantum non-Markovianity: Characterization, quantification and detection, Rep. Prog. Phys. **77**, 094001 (2014).

[7] B. H. Liu, L. Li, Y. F. Huang, C. F. Li, G. C. Guo, E. M. Laine, H. P. Breuer, and J. Piilo, Experimental control of the transition from Markovian to non-Markovian dynamics of open quantum systems, Nat. Phys. **7**, 931 (2011).

[8] F. F. Fanchini, G. Karpat, B. Çakmak, L. K. Castelano, G. H. Aguilar, O. Jiménez Farías, S. P. Walborn, P. H. Souto Ribeiro, and M. C. de Oliveira, Non-Markovianity through Accessible Information, Phys. Rev. Lett. **112**, 210402 (2014).

[9] N. K. Bernardes, A. Cuevas, A. Orieux, C. H. Monken, P. Mataloni, F. Sciarrino, and M. F. Santos, Experimental observation of weak non-Markovianity, Sci. Rep. **5**, 17520 (2015).

[10] S. Yu, Y. T. Wang, Z. J. Ke, W. Liu, Y. Meng, Z. P. Li, W. H. Zhang, G. Chen, J. S. Tang, C. F. Li, and G. C. Guo, Experimental Investigation of Spectra of Dynamical Maps and their Relation to Non-Markovianity, Phys. Rev. Lett. **120**, 060406 (2018).

[11] D. F. Urrego, J. Flórez, J. Svozilík, M. Nuñez, and A. Valencia, Controlling non-Markovian dynamics using a light-based structured environment, Phys. Rev. A **98**, 053862 (2018).

[12] M. Wittemer, G. Clos, H. P. Breuer, U. Warring, and T. Schaetz, Measurement of quantum memory effects and its fundamental limitations, Phys. Rev. A **97**, 020102(R) (2018).

[13] S. Cialdi, M. A. C. Rossi, C. Benedetti, B. Vacchini, D. Tamascelli, S. Olivares, and M. G. A. Paris, All-optical quantum simulator of qubit noisy channels, Appl. Phys. Lett. **110**, 081107 (2017).

[14] Z. D. Liu, H. Lyyra, Y. N. Sun, B. H. Liu, C. F. Li, G. C. Guo, S. Maniscalco, and J. Piilo, Experimental implementation of fully controlled dephasing dynamics and synthetic spectral densities, Nat. Commun. **9**, 3453 (2018).

[15] E.-M. Laine, J. Piilo, and H.-P. Breuer, Witness for initial system-environment correlations in open-system dynamics, Europhys. Lett. **92**, 60010 (2010).

[16] A. Smirne, H. P. Breuer, Jyrki Piilo, and B. Vacchini, Initial correlations in open-systems dynamics: The Jaynes-Cummings model, Phys. Rev. A **82**, 062114 (2010).

[17] M. Gessner and H. P. Breuer, Detecting Nonclassical System-Environment Correlations by Local Operations, Phys. Rev. Lett. **107**, 180402 (2011).

[18] C. F. Li, J. S. Tang, Y. L. Li, and G. C. Guo, Experimentally witnessing the initial correlation between an open quantum system and its environment, Phys. Rev. A **83**, 064102 (2011).

[19] A. Smirne, D. Brivio, S. Cialdi, B. Vacchini, and M. G. A. Paris, Experimental investigation of initial system-environment correlations via trace-distance evolution, Phys. Rev. A **84**, 032112 (2011).

[20] J. Dajka and J. Łuczka, Distance growth of quantum states due to initial system-environment correlations, Phys. Rev. A **82**, 012341 (2010); J. Dajka, J. Łuczka, and P. Hänggi, Distance between quantum states in the presence of initial qubit-environment correlations: A comparative study, *ibid.* **84**, 032120 (2011).

[21] D. Z. Rossatto, T. Werlang, L. K. Castelano, C. J. Villas-Boas, and F. F. Fanchini, Purity as a witness for initial system-environment correlations in open-system dynamics, Phys. Rev. A **84**, 042113 (2011).

[22] E. M. Laine, H. P. Breuer, J. Piilo, C. F. Li, and G. C. Guo, Nonlocal Memory Effects in the Dynamics of Open Quantum Systems, Phys. Rev. Lett. **108**, 210402 (2012).

[23] C. A. Rodríguez-Rosario, K. Modi, L. Mazzola, and A. Aspuru-Guzik, Unification of witnessing initial system-environment correlations and witnessing non-Markovianity, Europhys. Lett. **99**, 20010 (2012).

[24] K. Modi, Operational approach to open dynamics and quantifying initial correlations, Sci. Rep. **2**, 581 (2012).

[25] S. Wißmann, B. Leggio, and H.-P. Breuer, Detecting initial system-environment correlations: Performance of various distance measures for quantum states, Phys. Rev. A **88**, 022108 (2013).

[26] M. Gessner, M. Ramm, T. Pruttivarasin, A. Buchleitner, H-P. Breuer, and H. Häffner, Local detection of quantum correlations with a single trapped ion, Nat. Phys. **10**, 105 (2014).

[27] M. Ringbauer, C. J. Wood, K. Modi, A. Gilchrist, A. G. White, and A. Fedrizzi, Characterizing Quantum Dynamics with Initial System-Environment Correlations, Phys. Rev. Lett. **114**, 090402 (2015).

[28] F. T. Tabesh, S. Salimi, and A. S. Khorashad, Witness for initial correlations among environments, Phys. Rev. A **95**, 052323 (2017).

[29] G. Amato, H. P. Breuer, and B. Vacchini, Generalized trace distance approach to quantum non-Markovianity and detection of initial correlations, Phys. Rev. A **98**, 012120 (2018).

[30] F. A. Pollock, C. Rodríguez-Rosario, T. Frauenheim, M. Paternostro, and K. Modi, Operational Markov Condition for Quantum Processes, Phys. Rev. Lett. **120**, 040405 (2018); Non-Markovian quantum processes: Complete framework and efficient characterization, Phys. Rev. A **97**, 012127 (2018).

[31] P. Taranto, F. A. Pollock, S. Milz, M. Tomamichel, and K. Modi, Quantum Markov Order, Phys. Rev. Lett. **122**, 140401 (2019); P. Taranto, S. Milz, F. A. Pollock, and K. Modi, Structure of quantum stochastic processes with finite Markov order, Phys. Rev. A **99**, 042108 (2019).

[32] A. A. Budini, Quantum Non-Markovian Processes Break Conditional Past-Future Independence, Phys. Rev. Lett. **121**, 240401 (2018); Conditional past-future correlation induced by non-Markovian dephasing reservoirs, Phys. Rev. A **99**, 052125 (2019).

[33] As usual, $P(b|a)$ denotes the conditional probability of b given a.

[34] See Supplemental Material at http://link.aps.org/supplemental/10.1103/PhysRevA.100.050301 for a detailed derivation or explanation.

[35] W. H. Zurek, Environment-induced superselection rules, Phys. Rev. D **26**, 1862 (1982).

[36] W. H. Zurek, Decoherence, einselection, and the quantum origins of the classical, Rev. Mod. Phys. **75**, 715 (2003).

[37] F. M. Cucchietti, J. P. Paz, and W. H. Zurek, Decoherence from spin environments, Phys. Rev. A **72**, 052113 (2005).

[38] For the sake of brevity, the standard tomography setup [39,40] is hidden in Fig. 1.

[39] D. F. V. James, P. G. Kwiat, W. J. Munro, and A. G. White, Measurement of qubits, Phys. Rev. A **64**, 052312 (2001).

[40] S. Yu, F. Albarrán-Arriagada, J. C. Retamal, Y.-T. Wang, W. Liu, Z.-J. Ke, Y. Meng, Z.-P. Li, J.-S. Tang, E. Solano, L. Lamata, C.-F. Li, and G.-C. Guo, Reconstruction of a photonic qubit state with reinforcement learning, Adv. Quantum Technol. **2**, 1800074 (2019).